

Adhesion and friction behavior between fluorinated carbon fibers and poly (vinylidene fluoride)

A. BISMARCK*[‡]

*Department of Chemical Engineering & Chemical Technology, Imperial College London, South Kensington Campus, London, SW7 2 AZ, UK
E-mail: a.bismarck@imperial.ac.uk*

E. SCHULZ

Lab. VI.21: "Micromechanics of Heterogeneous Polymers and Composites/Interphases-Interfaces," Bundesanstalt für Materialforschung und-prüfung (BAM), Unter den Eichen 87, D-12205 Berlin, Germany

The potential use of fluorinated, polyacrylonitrile-based, high strength carbon fibers as reinforcement for a fluorocarbon polymer, namely poly (vinylidene fluoride) (PVDF), was investigated by means of the single fiber pull-out test. The apparent interfacial shear strength as a measure of practical adhesion was determined and the fracture and friction behavior of the model composites characterized.

It was shown that the fracture behavior of the model composites is predominately brittle in nearly all cases. Fluorination of carbon fibers has a positive impact on the adhesive strength to PVDF. The apparent interfacial shear strength increases with increasing degree of fiber surface fluorination and becomes maximal at a degree of fiber fluorination (F/C-ratio) of around 0.8, determined by ESCA, which is close to that of PVDF. This result points to the fact that the increased "practical" adhesion is due to a physical compatibilization between the fluorinated fibers and the surrounding PVDF matrix. It was found that, even though the interfacial shear strength increases with increasing degree of fiber surface fluorination, the friction between fluorinated carbon fibers and the surrounding PVDF decreases. © 2003 Kluwer Academic Publishers

1. Introduction

Fibre reinforced polymers (FRP) are able to provide a beneficial balance between the traditional properties of a polymer (low part weight and ease of processability) and selective properties of metals (high strength, modulus and toughness). FRPs allow tailoring of unique combinations of such properties to meet practical and design requirements. Thermoplastic polymers find increasing interest in the sector of FRPs due to shorter cycling times, recycleability, and due to the increased safety demands at the workplace. Since thermoplastics display relatively high elongations to fracture, the excellent properties of carbon fiber reinforcements become more apparent in thermoplastic composite materials. In addition they offer a high tolerance against impact damage and a good resistance against various chemicals [1, 2].

Fluoropolymers are of huge technological and industrial importance due to their abrasion resistance,

thermal stability, chemical barrier and electrical insulating properties, and outstanding chemical inertness [3]. In their natural state many such polymers are already amongst the strongest and stiffest thermoplastics [4]. Polyvinylidene fluoride (PVDF) is used since the early 1960s because of its excellent resistance to chemicals (however, since it contains also carbon-hydrogen bonds it is not as chemically inert as other fluorocarbon polymers, like for instance PTFE) and irradiative attacks in combination with very good mechanical properties (very low creep and high mechanical strength) [5–8]. PVDF possesses a remarkable thermal stability under operating and processing application temperatures and is not flammable. This enables the use of PVDF from -40°C up to temperatures of 150°C (manufactures claim) in air [8, 9]. Additionally, PVDF has valuable piezoelectric and pyroelectric properties [10]. Because of its superb weathering and exterior properties as well as low water adsorption (0.03 to 0.06%

*Author to whom all correspondence should be addressed.

[‡]At the time the study was performed A.B. was employed by: Sulzer Composites, Sulzer Markets & Technology Ltd., Zürcherstr. 58, CH-8401 Winterthur, Switzerland. Sulzer Composites is now Gurit Suprem.

increase by weight) PVDF is often used as protective barrier coatings [11].

The offshore oil and gas industry continues developing deep-sea oilfields. The extreme conditions encountered in such operations require superior material performance and durability. The materials have to withstand combined severe service conditions, aggressive media (sweet and sour well fluids), high abrasion, high but fluctuating working temperatures, pressure differences and mechanical load. Conventionally used engineering materials have exhausted their potential because of the high costs involved in supporting their own weight. Polymer composites can overcome such limitations, thus enabling new design strategies for cost effective, weight and energy saving materials. Heavy metal pipes used as risers, flowlines and choke and kill lines will have to be replaced by non-corroding and lighter alternative materials in the near future. Spoolable reinforced thermoplastic pipes [12] have been developed to transport highly corrosive fluids, including crude oil, brine and sour gases at high service pressures. For these applications PVDF is currently the premium polymeric sheath material (the only available above 90°C) with an upper service temperature limit of 130°C [13].

In thermoplastic composites, however, it can be more difficult to guarantee the required interfacial adhesion as compared to thermosetting matrices. The combinations of rather high melt viscosities and moreover the lack of 'reactive' groups in thermoplastics causes difficulties in fiber impregnation and to form attractive ('chemical') bonds to surface functionalities of the reinforcing material. Thus other 'specific' interactions are necessary to achieve the desired adhesive strength. Typically the interactions are of acid-base type (including hydrogen bonding). In addition to the specific interactions mechanical interlocking might also contribute to the adhesion [14].

The combination of the superior properties of carbon fibers [15] (very high specific properties, i.e., stiffness and strength) with the above-mentioned properties of fluorocarbon polymers in fiber-reinforced composites is a very challenging task. However, the low ability of fluorocarbon polymers to form adhesive bonds makes it rather difficult to succeed. Commonly there are two possibilities to improve adhesion between the adherent and adhesive; (i) to modify the reinforcing fibers and (ii) to modify the surrounding matrix material. In the literature many reports on the surface modification of fluorocarbon polymers aiming to improve the adhesion behavior can be found. Such polymer surface modifications include chemical etching [16], high-energy irradiation techniques [17, 18] and plasma treatments [19]. However, since polymer surface modifications rendering the surfaces more hydrophilic are not stable with time (the phenomenon is often called hydrophobic recovery) [20], therefore we decided to modify the carbon fiber surfaces aiming to compatibilize carbon fibers to a fluorocarbon polymer.

Despite the large body of research on many aspects of fiber surface modifications and their impact on adhesion, there is very little published work into fiber/fluoropolymer interactions and fluoropolymer

composite performance. The only academic study is by Loh *et al.* [21] who briefly described that plasma fluorination of carbon fibers offers the possibility to improve the macromechanical performance of fluorinated carbon fiber filled fluoroplastic (fluorinated ethylene propylene (FEP) and perfluoroalkoxyethylene (PFA)) composites, through enhanced physical compatibility. The most recent, available literature, dating back to 1998, is limited mainly to patents. They [22] claim processes to make fluoropolymer/fiber composites using all kinds of fibers, including graphite and fluorinated graphite fibers.

Commercially available carbon fibers are usually oxidized and sized. However, most fiber sizings are hardly compatible with thermoplastic polymers and even less suitable for fluoropolymers. To overcome this problem, fiber manufacturers recommend the use of unsized carbon fibers as reinforcement for fluoropolymers. Still, the use of such fibers *does not* lead to the best composite performance due to the subsequently weak fiber/matrix strength. Currently, there is a pressing need for more information on the physical and chemical mechanisms responsible for fiber-to-thermoplastic matrix adhesion.

Knowing that PVDF is amongst the strongest and stiffest thermoplastics in its natural state [4] begs the question, as to whether the full potential of PVDF has yet been exploited. It is clear that there is still a significant body of knowledge to be built, regarding the improvement of the mechanical properties of this class of polymers. A major option for the use of such polymers as the matrix material for unidirectional FRPs has yet to be realized. In the present study carbon fibers were used that were modified by direct fluorination [23]. In the present study we will focus on the micromechanical adhesion behavior between fluorinated carbon fibers to a surrounding PVDF matrix as investigated using the single fiber pull-out test. In previous studies we investigated the influence of the fluorination on the fiber surface composition and bulk structure [23] as well as physical-chemical surface properties [24].

1.1. Theoretical considerations to adhesion

A basic requirement of adhesion is the intimate contact between the phases (here, the reinforcing fiber and the polymeric matrix), as well as the formation of a cohesively strong solid of the matrix material [25]. From the thermodynamic point of view, the better the wetting between the molten adhesive and the adherend the better the adhesion¹ [26]. This would be indicated by a lower contact angle between the adhesive and substrate. In order to establish intimate contact between the reinforcement and the 'liquid' matrix material, the liquid matrix should not be too viscous, and there should be a thermodynamic driving force which affects good wettability [27]. This driving force can be expressed by the thermodynamic work of adhesion W_a , which is the work required to reversibly separate two bulk phases from their equilibrium separation distance. W_a is the sum of

¹ Definition: "Thermodynamic adhesion refers to equilibrium interfacial forces or energies associated with reversible processes" [26].

all the interaction energies between the two phases.

$$W_a = \gamma_s + \gamma_l - \gamma_{sl} \quad (1)$$

For the adhesion of liquids which do not completely spread on the solid surface (e.g., a polymer melt), the Young-Dupré equation should be valid:

$$W_a = \gamma_l \cdot (1 + \cos \theta). \quad (2)$$

where θ represents the equilibrium or Young-contact angle. Unfortunately direct measurements of contact angles of polymer melt droplets on thin fibers [28] are still quite difficult and, therefore, an indirect method was applied to estimate the surface tension of the fibers as well as the polymer.

There are different approaches commonly used to estimate the thermodynamic work of adhesion from the surface tension (and its components or parameters) estimated from contact angle data of test liquids with known surface tension (components) [26, 29, 30]. However, the literature contains important critique on the various approaches to determine solid surface tensions from contact angle data. Fowkes *et al.* [31] disputed the possibility to obtain correct values for the solid surface tensions from contact angle measurements in principal. Kwok *et al.* [32–35] raised critique on the suitability of the polar/dispersive [26] as well as the acid/base approach [36] in order to determine interfacial or surface tensions from measured contact angles. They claim that contact angles do not contain any information about assumed polar/dispersive nor acid/base surface tension components and that all other surface tension components theories are untenable. And finally, Makkonen [37] stated that all theories to obtain solid surface tensions from measured contact angles might be incorrect.

Contact angle measurements are far from trivial and the accuracy of the surface tension to be determined is strongly dependent on the quality of the contact angle data. Since our primary aim is to optimize the adhesive interactions between reinforcing fibers and PVDF we have decided to use the most recent and so far unchallenged Kwok approach.

2. Experimental

2.1. Materials

The fibers used in this study were two polyacrylonitrile (PAN) based high tensile strength (HT) carbon fibers C320.00A (CA) (kindly supplied by Sigri SGL Carbon, Meitingen, Germany) and Torayca T 300 (T) (FT 300 6000-99, form Toray Industries, Tokyo, Japan). The various fluorinating agents and the experimental procedure are described in [23].

The commercial PVDF material Kynar[®] 711 in powder form was kindly supplied by Atofina (Serquigny, France).

2.2. Contact angle measurements

In order to estimate the PVDF surface tension ‘static advancing’ contact angles against various test liquids

with known surface tensions and surface tension components (water, diiodomethane (DIM), formamide and α -bromonaphthalene) were measured on a Kynar 720 Mono-layer (50 μm) film² (Atofina (Schweiz) AG, Stallikon, Switzerland) using the sessile drop method applied in the Krüss DSA10 at room temperature (RT = 20°C). The measurements were taken immediately after the droplets were placed from above on the film surface. A microsyringe was used to form the droplets. At least 10 readings were taken for different drops placed on several spots of the surface.

2.3. Adhesion between carbon fibers and the PVDF matrix: single fiber pull-out test

The ‘single fiber composites’ for the pull-out tests were prepared in a special embedding machine, which allows a fiber orientation exactly perpendicular to the matrix surface at a defined embedded fiber length [38]. A fiber was partially embedded in a polymer melt droplet on an aluminum sample carrier. Specimens were prepared as follows: At a temperature of 260°C the carbon fibers were embedded in a polymer melt droplet with a determined length between 50–200 μm . After embedding the fiber, the whole sample was cooled down to room temperature with air in about 2 min. After specimen preparation, every fiber diameter was measured using a laser diffraction method [39].

Pull-out experiments were performed with a home made apparatus with a high stiff frame to avoid energy storage in the device itself and mainly in the free fiber length ($l_f = 30 \mu\text{m}$) between the matrix surface and the clamping mechanism [40]. The fiber pull-out was performed at a constant speed of 0.2 $\mu\text{m/s}$ from the matrix using a controlled load cell. Pull-out load against displacement was recorded using a computer controlled plotter.

The apparent shear strength τ_{IFSS} was calculated from the maximum pull-out force F_{max} and fiber embedded area in the matrix using the mathematical relation,

$$\tau_{\text{IFSS}} = \frac{F_{\text{max}}}{\pi d_f L} \quad (8)$$

where L is the embedded length and d_f is the fiber diameter.

Further details on the fiber pull-out technique can be found in [41].

3. Results and discussion

First, we want to summarize what we know already about the fluorinated carbon fibers used in this study. It is known that fluorine is able to form different kinds of chemical bonds with carbon materials. The interactions between C and F can vary from covalent, through semi-ionic, to ionic [42, 43] and even van der Waals interactions can also be of importance [43]. The variety of different C–F bonds that can be formed will,

²No Kynar 710 film is available, the only difference between Kynar 710 or 711 (powder form) and Kynar 720 is a higher molecular mass and therefore higher melt viscosity.

TABLE I F/C-ratio of the carbon fibers determined using ESCA [23], advancing θ_a and receding θ_r contact angles against water and diiodomethane (DIM) as well as the fiber surface tension (γ_f) calculated from measured advancing contact angles using the Neumann's equation-of-state approach [44]

| Fiber | F/C-ratio | $\theta_a^{\text{H}_2\text{O}} / ^\circ$ | $\theta_r^{\text{H}_2\text{O}} / ^\circ$ | $\theta_a^{\text{DIM}} / ^\circ$ | $\theta_r^{\text{DIM}} / ^\circ$ | γ_f (mN/m) |
|-------|-----------|--|--|----------------------------------|----------------------------------|-------------------|
| CA | 0 | 82.5 ± 2.9 | 56.3 ± 3.1 | 49.5 ± 3.2 | 47.7 ± 3.2 | 35.2 ± 1.8 |
| C1 | 0.5 | 62.4 ± 3.5 | 40.1 ± 5.8 | 58.8 ± 3.0 | 40.4 ± 1.1 | 39.2 ± 10.2 |
| C2 | 0.8 | 69.9 ± 4.8 | 37.3 ± 4.4 | 62.7 ± 2.1 | 37.2 ± 1.8 | 35.9 ± 8.3 |
| C3 | 1.8 | 92.3 ± 12.5 | 54.5 ± 10.4 | 66.5 ± 5.9 | 33.2 ± 4.6 | 28.0 ± 0.3 |
| C4 | 0.6 | 73.2 ± 2.4 | 40.8 ± 5.6 | 57.3 ± 1.1 | 40.8 ± 1.3 | 36.2 ± 5.0 |
| C5 | 1.5 | 91.7 ± 12.5 | 46.8 ± 11.4 | 62.5 ± 5.0 | 35.3 ± 6.6 | 29.2 ± 1.4 |
| T | 0 | 80.3 ± 1.0 | 47.2 ± 1.5 | 33.7 ± 1.4 | 19.8 ± 2.7 | 39.3 ± 5.6 |
| T2 | 0.1 | 83.2 ± 5.2 | 55.9 ± 4.9 | 59.1 ± 4.1 | 55.0 ± 2.3 | 32.7 ± 1.2 |

TABLE II Static advancing contact angles of four different test liquids measured on PVDF shortly (about 2 s) after the drops were placed onto the sample

| Test liquids | Water | Formamide | Diiodomethane | α -Bromonaphthalene |
|---------------------------------|------------|------------|---------------|----------------------------|
| γ_f (mN/m) | 72.8 | 58.2 | 50.8 | 44.6 |
| θ_a ($^\circ$) on PVDF | 81.9 ± 2.4 | 61.3 ± 2.6 | 56.2 ± 2.6 | 39.7 ± 2.4 |

however, affect the surface character of the fluorinated carbon surface. If covalent C–F_x bonds are predominantly formed the resulting fiber surfaces will turn more hydrophobic, whereas the formation of ionic C⁺···F[−] bonds will render the modified fiber surfaces slightly more hydrophilic. However, even if covalent C–F bonds are formed, surfaces can become more hydrophilic because of the polarization effect of an on C bonded F-atom to the neighboring C-atom, which then can be attacked by and bond air oxygen easier [45]. As expected, at a higher degree of surface fluorination the fibers become more hydrophobic, i.e., the water contact angles increase.

The water contact angle data for the fluorinated CA indicate that a slight fluorination until a F/C-ratio of 1 (obtained from ESCA-measurements [23]) increases the wettability of the fluorinated fibers (Table I). Beyond a F/C-ratio of 1 the water contact angles increase, i.e., the hydrophobic character increases. For the investigated T-fibers the increasing contact angles with increasing F-content indicate an increased degree of hydrophobicity. The fiber surface tensions γ_f were calculated from the measured dynamic advancing contact angles using Neumann's equation of state approach [44] and are also presented in Table I. As can be seen, the surface tension of the CA fibers is initially increasing up to a maximum with increasing degree of fluorination. Further increase of the degree of fluorination causes the surface tension to decrease. In case of the T-fibers the surface tension just decreases drastically even at a low degree of fluorination. The estimated fiber surface tensions clearly show that the accuracy of values depends strongly on the quality of the contact angle data. However, if the contact angles approach or even exceed 90° the more difficult it becomes to immerse, to force the thin fibers into the test liquid making it even harder to determine high quality contact angles required for calculate solid surface tensions. Measured time-dependent ζ -potentials [24] reflect the surface composition of the fluorinated carbon fiber material due to the dissociation of ionic C⁺···F_x[−] ($x = 1-3$) groups. Fibers containing ionic C⁺···F[−] bonds reveal the lowest negative

zeta (ζ) potentials, in case of semi-ionic bonded F the interpretation is more difficult. Half of the 'semi-ionic' fibers exhibit a low negative ζ -potential and the others the greatest negative ζ -values, this might be caused by only a smaller content of ionic-bonded F. The pH-dependence of the ζ -potential of all investigated carbon fibers clearly shows an increased acidic character of the fluorinated carbon fibers compared to the original untreated fibers.

In contrast to many oxidative fiber surface treatments a slight fluorination will not affect the intrinsic fiber mechanical properties, the tensile strength and E -modulus [45, 46]. Therefore, slight fluorination might be a possibility in order to improve the interaction between carbon fibers and fluorocarbon polymers, while keeping the fiber properties as they are for pristine fibers.

However, as we know from our previous study [23] in case of the strongly fluorinated fiber C3, the formation of a stage 3 C_xF compound was confirmed. This treatment resulted in fibers with increased fiber diameter (see also Table III) and might surely lead to changed mechanical fiber properties.

3.1. What adhesion behavior could we expect?

Commonly, the work of adhesion W_a of an imaginary polymer/fiber combination is used to estimate a trend of adhesion. We use the most recent approach to estimate W_a . Here, we use the estimated solid surface tensions to calculate W_a using Kwok's approach [30]. In order to determine the surface tension of PVDF, 'static' advancing contact angles were measured for various test liquid droplets resting on the PVDF film (Table II). All contact angle data³ were used to calculate the polymer (solid) surface tension using the equation-of-state (eos) and acid/base approach. The surface tension of PVDF using the eos-approach is $\gamma_{\text{PVDF}}^{\text{eos}} = 34.8 \pm 1.2$ mN/m

³Plotting experimental wetting tension $\gamma_v \cos \theta$ values over the liquid surface tension γ_v values results in the expected smooth curves always reported by Neumann *et al.*

TABLE III Measured fiber diameters (d_f) and apparent interfacial shear strength (τ_{IFSS})

| Fiber | d_f (μm) | τ_{IFSS} (MPa) |
|-------|-------------------------|----------------------------|
| CA | 7.0 ± 0.5 | 27.7 ± 1.7 |
| C1 | 7.3 ± 0.5 | 26.7 ± 1.7 |
| C2 | 7.7 ± 0.6 | 34.9 ± 2.9 |
| C3 | 8.7 ± 0.2 | 28.0 ± 3.0 |
| C4 | 7.7 ± 0.5 | 26.0 ± 1.1 |
| C5 | 6.5 ± 0.5 | 33.7 ± 1.4 |
| T | 7.0 ± 0.4 | 27.7 ± 1.8 |
| T2 | 7.4 ± 0.5 | 21.1 ± 0.9 |

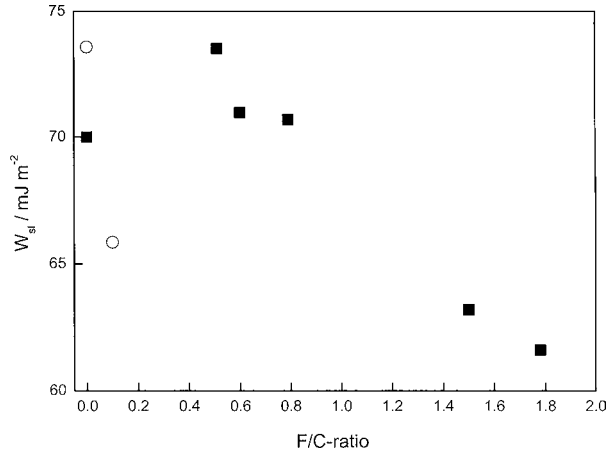


Figure 1 Work of adhesion for the imaginary system (fluorinated) CA and T carbon fibers as calculated using Kwok's approach [30] as function of the degree of fiber surface fluorination F/C.

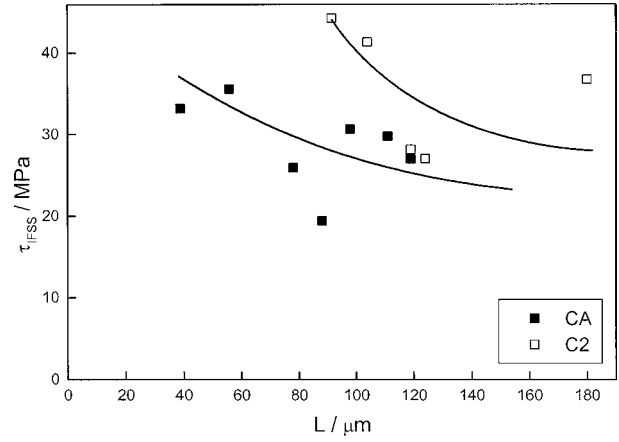
and using the acid/base approach we obtain the following surface tension $\gamma_{\text{PVDF}} = 36.0 \pm 2.6$ mN/m consisting of the Lifshitz/van der Waals component $\gamma_{\text{PVDF}}^{\text{LW}} = 33.6 \pm 0.86$ mN/m and an acid/base of only $\gamma_{\text{PVDF}}^{\text{ab}} = 2.4 \pm 1.7$ mN/m. The acid and base parameters of the surface tension are: $\gamma_{\text{PVDF}}^+ = 0.25 \pm 0.27$ mN/m and $\gamma_{\text{PVDF}}^- = 5.60 \pm 2.2$ mN/m, respectively. Even though, the assumptions made to determine the surface tension from contact angle data as different as it can get, the values are still in quite good agreement. Furthermore, the PVDF surface tension estimated are in good agreement to the re-calculated value from the contact angles reported by Wu [26]: $\gamma_{\text{PVDF}} = 33.3$ mN/m, $\gamma_{\text{PVDF}}^{\text{d}} = 28.1$ mN/m and $\gamma_{\text{PVDF}}^{\text{p}} = 5.2$ mN/m, $X^{\text{P}} = 0.16$.

The W_a values calculated using Kwok's approach for an imaginary combination of fluorinated carbon fibers and PVDF is shown in Fig. 1. If the practical adhesion is directly proportional to W_a we would expect that it increases for fluorinated fibers. The practical adhesion should increase up to a maximum at degree of fluorination of around $F/C \approx 0.5$ to decrease further with increasing degree of fluorination.

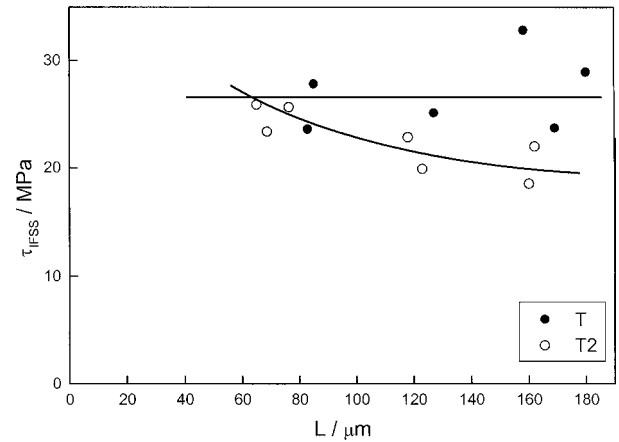
3.2. Adhesion between fluorinated carbon fibers and PVDF

In this section we want to focus on the fracture and adhesion behavior between the fluorinated carbon fibers and the PVDF-matrix.

Fig. 2 shows the results of the measured apparent shear strength between original and fluorinated carbon



(a)



(b)

Figure 2 (a) Apparent interfacial shear strength τ_{IFSS} as function of the embedded fiber length L for the original CA and fluorinated C2 fibers. (b) Apparent interfacial shear strength τ_{IFSS} as function of the embedded fiber length L for the original T and fluorinated T2 fibers.

fibers and the PVDF matrix as function of the embedded fiber length observed by the single fiber pull-out test. The lines in the figure should be taken only as trend indicator and, therefore, they do not represent any data fitting. From these trends, it is possible to characterize the fracture behavior of a 'single fiber composite.' According to Hampe *et al.* [40]; the apparent shear strength does not depend on the embedded fiber length a predominately ductile fracture behavior occurs during the pull-out process. On the other hand, an almost non-linear dependence of the apparent shear strength with increasing embedded fiber length would represent a brittle failure behavior.

As can be seen in Fig. 2 (Fig. 2a, exemplarily shown for the original CA and the fluorinated C2 fiber; Fig. 2b for original T and fluorinated T2 fibers) the measured apparent interfacial shear strength between almost all investigated fiber PVDF composites is dependent on the embedded fiber length, i.e., the interfacial shear strength decreases with increasing embedded fiber length, indicating a brittle fracture behavior of the composites. However, in case of the pristine Toray T300 fibers, the fiber/PVDF interface failed in a predominately ductile manner (no dependence between the apparent shear strength and the embedding length (see Fig. 2b) on a higher strength level than that of the fluorinated T2 fibers, whereas the behavior of the fluorinated

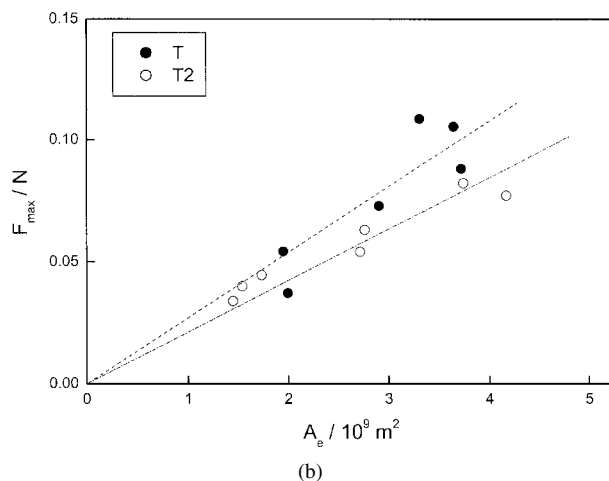
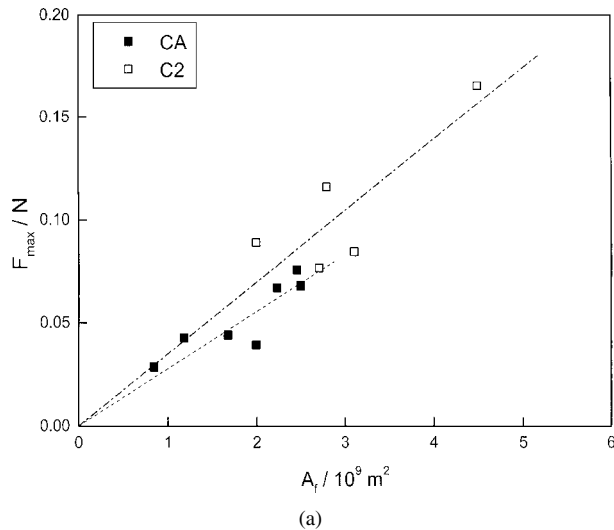


Figure 3 (a) The maximum pull-out force F_{\max} as function of the embedded fiber area A_f for the original CA and fluorinated C2 fibers. (b) The maximum pull-out force F_{\max} as function of the embedded fiber area A_e for the original T and fluorinated T2 fibers.

C-fiber composites was vice versa. The typically observed pull-out force-displacement curves show that the measured force increases until its maximum and drops more or less suddenly after the debonding is completed to a lower value. After debonding is completed, continuing the pull-out experiment the force then decreases further with proceeding fiber pull-out and is controlled by the friction between the fiber and polymer.

Fig. 3 presents (exemplarily) the measured pull-out forces between the pristine carbon fibers (CA) as well as the fluorinated fibers C2 and the PVDF matrix as a function of the embedded fiber/matrix area A_e . According to Subramanian *et al.* [47] the slope of the pull-out force as function of the embedded fiber area represents the strength of adhesion, that is the apparent interfacial shear strength τ_{IFSS} . As can be seen from Fig. 3 the linearly fitted experimental data, the maximum force versus embedded fiber area, pass through the origin of the graph. Even though, the two carbon fiber samples follow a similar trend, the slopes of the lines are different indicating a change in the adhesion strength for the pristine and fluorinated carbon fibers. Table III summarizes the determined apparent interfacial shear strength for all investigated fibers. As can be seen from the data in Table III most determined apparent interfacial shear

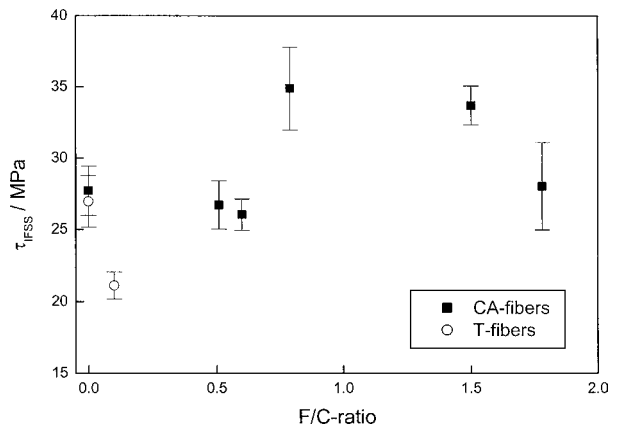


Figure 4 Measured apparent interfacial shear strength τ_{IFSS} as function of the degree of fiber surface fluorination, expressed as F/C-ratio as determined using ESCA.

strength for the pristine and fluorinated carbon fibers are quite similar except for the fluorinated fibers C2, C5 and T2. For the two fluorinated CA-fibers an increase in τ_{IFSS} of 25.8% and 21.6% (Fig. 4), respectively, was measured. In case of the fluorinated T-fibers, a reverse behavior could be detected with a decrease in τ_{IFSS} of 21.6% (Fig. 4).

The presented experimental data show that a fluorination of carbon fibers will not result in an improved adhesion behavior in all cases. However, the trend of the changing practical adhesion as function of the degree of fluorination (Fig. 4) follows the predicted trend (Fig. 1). The measured apparent interfacial shear strength τ_{IFSS} increases up to a maximum at a degree of fiber surface fluorination of about $F/C \approx 0.8$. Atofina, the manufacturer of the used PVDF states that the polymer contains approximately 59% fluorine [8]. The F/C-ratio determined using ESCA for PVDF is approx. $F/C \approx 0.85^4$ [19]. The reason for the improved adhesion could be the improved physical compatibilization (an almost equal F/C-ratio) between the fluorinated fibers and the PVDF matrix.

3.3. Fiber/matrix friction

In a previous study it was stated that the fluorination of carbon fibers is lowering the coefficient of friction in fluorocarbon composites [48]. The performed single fiber pull-out experiments on (fluorinated) carbon fiber/PVDF model composites also allow at least a qualitative characterization of the friction behavior between the fibers and the PVDF matrix after fiber debonding is completed. After completed fiber debonding the force decreases further, with proceeding fiber pull-out up to the complete separation of fiber and matrix. A qualitative measure for the fiber/matrix friction can be obtained by evaluating the slope of the pull out curve ($\Delta F / \Delta A_f$) in this part of the pull-out experiment.

In order to evaluate the friction behavior between the non- and fluorinated carbon fiber/PVDF composites, the last part of the pull-out force-displacement

⁴The PVDF used in the quoted study was also a Kynar-grade film from Atofina.

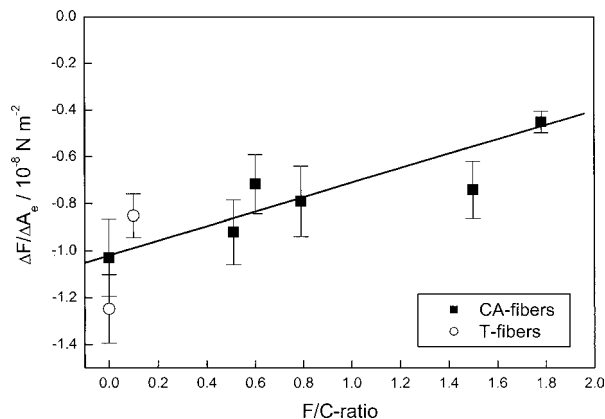


Figure 5 Friction behavior between fluorinated carbon fibers and PVDF as function of the degree of fiber surface fluorination. The friction is characterized as change in pull-out force after complete debonding as function of the decreasing embedded fiber area ($\Delta F/\Delta A_f$).

curves were converted into pull-out force-embedded fiber area curves. This was possible since the fiber diameter of each tested specimen was determined separately prior to each measurement. The linear part of the force-displacement curve after the debonding peak (F_{max}) was fitted for all pull-out experiments. The slope $\Delta F/\Delta A_f$ is a qualitative measure for the fiber/matrix friction behavior. The results are shown in Fig. 5 (the error bars shown are the resulting standard deviations of the mean averaged values). As can be seen the slope $\Delta F/\Delta A_e$ is a function of the F/C-ratio and decreases linearly from an averaged value for both pristine fibers in the range of $\Delta F/\Delta A_e = -1.1 \times 10^8 \text{ N/m}^2$ with increasing degree of surface fluorination. This is surprising, considering that the 'practical' adhesion between the fluorinated fibers and PVDF increases up to a F/C-ratio of 0.8.

4. Concluding remarks

The influence of carbon fiber surface fluorination over a wide range $0 < F/C < 1.8$ on the adhesion and fracture behavior of single fiber PVDF-composites has been studied using the single fiber pull-out test. It was shown that the fracture behavior of the model composites is in nearly all cases, except for the pristine T300 fiber, predominately brittle. The fluorination of carbon fibers has a positive impact on the measurable adhesive strength; the apparent interfacial shear strength. The interfacial shear strength increases with increasing degree of fiber surface fluorination to become maximal at a F/C-ratio of around 0.8, which corresponds to the surface F/C-ratio of PVDF. This points to the fact that the increased adhesion is due to an improved physical compatibilization between the fluorinated fibers and the surrounding PVDF matrix. The trend of the changing practical adhesion as function of the degree of fluorination follows the same trend as predicted from work of adhesion values calculated using Kowk's equation of state approach.

Finally, the friction behavior between the fluorinated carbon fibers and the surrounding PVDF matrix was characterized qualitatively. It was found that the slope of the force-displacement curve after fiber/matrix

debonding ($\Delta F/\Delta A_f$) decreases linearly with increasing degree of fiber fluorination, even though the fiber/matrix adhesion increases up to a maximum.

Acknowledgement

We are very grateful to Frau Martina Bistriz (BAM-Berlin) for her valuable help conducting the experimental fiber pull-out testing work.

References

1. K.-H. SPRENGER, in "Faserverbundwerkstoffe mit thermoplastischer Matrix; Hochleistungswerkstoffe für Rationelle Verarbeitung," edited by H.-P. Zempf (Expert Verlag, Renningen-Malmsheim, 1997).
2. G. KEMPE, in "Faserverbundwerkstoffe mit thermoplastischer Matrix; Hochleistungswerkstoffe für Rationelle Verarbeitung," edited by H.-P. Zempf (Expert Verlag, Renningen-Malmsheim, 1997).
3. J. G. DROBNY, *Macromol. Symp.* **170** (2001) 149.
4. J. R. F. ANDREWS and M. BEVIS, *J. Mater. Sci.* **19** (1984) 653.
5. *Idem.*, *ibid.* **19** (1984) 645.
6. D. L. KERBOW and C. A. SPERATI, in "Polymer Handbook," 4th ed. edited by J. Brandrup, E. H. Immergut and E. A. Grulke (John Wiley & Sons, New York, 1999) p. V/31.
7. J. D. MUZZY, in "Polymer Matrix Composites," Vol. 2 edited by R. Talreja and J.-A. Manson; "Comprehensive Composite Materials," edited by A. Kelly and C. Zweben (Pergamon, Amsterdam, 2001).
8. ATOFINA, "Product Information Kynar®," in link: <http://www.atofina.com/groupe/gb/solutions/produits/informarque.cfm?IdMarque=217> accessed on 07.12.2001.
9. MatWeb, in link: <http://www.matweb.com/SpecificMaterial.asp?bassnum=PAT105&group=General> accessed on 07.12.2001.
10. W.-T. WHANG and W.-H. CHENG, *Polym. Engin. Sci.* **35** (1995) 666.
11. R. A. IEZZI, S. GABOURY and K. WOOD, *Prog. Org. Coat.* **40** (2000) 55.
12. H. LÜHRSEN, *3R International* **40** (2001) 46.
13. B. THOMSON, M. V. LEWAN and R. P. CAMPION, in "Oilfield Engineering with Polymers" (Conference Proceedings, Rapra Technology Ltd., 2001).
14. I. K. ISMAIL and M. D. VANGSNES, *Carbon* **26** (1988) 749.
15. A. SHINDO, in "Fiber Reinforcements and General Theory of Composites," Vol. 1 edited A. Kelly and C. Zweben; "Comprehensive Composite Materials," edited by A. Kelly and C. Zweben (Pergamon, Amsterdam, 2001).
16. D. W. DWIGHT and W. M. RIGGS, *J. Coll. Interf. Sci.* **47** (1974) 650.
17. A. LE MOEL, J. P. DURAUD, C. LE COMPTE, M. T. VALIN, M. HENRIOT, C. DARNEZ, E. BALANZAT and C. M. DEMANET, *Nucl. Instrum. Meth. B* **32** (1988) 115.
18. J. P. DURAUD, A. LE MOEL, N. BETZ, A. FINA and E. BALANZAT, *Rad. Eff. Def. Solids* **110** (1989) 33.
19. M. D. DUCA, C. L. PLOSCEANU and T. POP, *Polym. Degrad. Stab.* **61** (1998) 65.
20. C. M. WEIKART and H. K. YASUDA, *J. Polym. Sci. A, Polym. Chem.* **38** (2000) 3028.
21. I. H. LOH, R. E. COHEN and R. F. BADDOUR, *J. Mater. Sci.* **22** (1987) 2937.
22. See for instance: C. K. DEAKYNE and G. P. WEEKS, US Patent no. 5,470,409 (1995); T. UENO and M. INAMORI, US Patent no. 5,705,120 (1998).
23. A. BISMARCK, R. TAHHAN, J. SPRINGER, A. SCHULZ, T. M. KLAPÖTKE, H. ZELL and M. MICHAELI, *J. Fluorine Chem.* **84** (1997) 127.
24. A. BISMARCK and J. SPRINGER, *Coll. Surf. A* **159** (1999) 331.
25. J. COMYN, "Adhesion Science" (RSC paperbacks, Cambridge, 1997).

26. S. WU, "Polymer Interface and Adhesion" (Marcel Dekker, New York, 1982).
27. D. HULL and T. W. CLYNE, "An Introduction to Composite Materials," 2nd ed (Cambridge University Press, Cambridge, 1996).
28. B. SONG, A. BISMARCK, R. TAHHAN and J. SPRINGER, *J. Coll. Inter. Sci.* **197** (1998) 68.
29. R. G. GOOD, M. K. CHAUDHURY and C. J. VAN OSS, in "Fundamentals of Adhesion," edited by L. H. Lee (Plenum Press, New York, 1991).
30. J. ZHANG and D. Y. KWOK, *Langmuir* **19** (2003) 4666.
31. F. M. FOWKES, F. L. RIDDLE, JR., W. E. PASTORE and A. A. WEBER, *Coll. Surf.* **43** (1990) 367.
32. D. Y. KWOK, D. LI and A. W. NEUMANN, *Langmuir* **10** (1994) 1323.
33. D. Y. KWOK and A. W. NEUMANN, *Can. J. Chem. Engin.* **74** (1996) 551.
34. D. Y. KWOK, Y. LEE and A. W. NEUMANN, *Langmuir* **14** (1998) 2548.
35. D. Y. KWOK and A. W. NEUMANN, *Progr. Coll. Polym. Sci.* **109** (1998) 170.
36. R. G. GOOD and C. J. VAN OSS, in "Modern Approached to Wettability Theory and Applications," edited by M. E. Schrader and G. Loeb (Plenum Press, New York, 1991).
37. L. MAKKONEN, *Langmuir* **16** (2000) 7669.
38. A. HAMPE and C. MAROTZKE, *Polym. Intern.* **28** (1992) 313.
39. S. MERETZ, T. LINKE, E. SCHULZ, A. HAMPE and M. HENTSCHEL, *J. Mater. Sci. Lett.* **11** (1992) 1471.
40. A. HAMPE, G. KALINKA, S. MERETZ and E. SCHULZ, *Composites* **26** (1995) 40.
41. L. T. DRZAL, P. J. HERRERA-FRANCO and H. HO, in "Test Methods, Nondestructive Evaluation and Smart Composites," Vol. 5, edited by L. A. Carlsson; "Comprehensive Composite Materials," edited by A. Kelly and C. Zweben (Pergamon, Amsterdam, 2001).
42. A. TRESSAUD, C. GUIMON, V. GUPTA and F. MOGUET, *Mater. Sci. Engin.* **B 30** (1995) 61.
43. H. TOUHARA and F. OKINO, *Carbon* **38** (2000) 241.
44. J. K. SPELT and D. LI, in "Applied Surface Thermodynamics," edited by A. W. Neumann and J. K. Spelt (Marcel Dekker, New York, 1996).
45. Y.-B. CHONG and H. OHARA, *J. Fluorine Chem.* **57** (1992) 169.
46. L. P. KOBETS, M. A. CHUBAROVA, D. K. KHAKIMOVA, N. V. POLYAKOVA and A. S. FIALKOV, *Mech. Composite Mater.* **1** (1981) 1.
47. R. V. SUBRAMANIAN, J. J. JAKUBOWSKI and F. D. WILLIAMS, *J. Adhesion* **9** (1978) 185.
48. "Graphite Reinforces Fluorocarbon Fibers," *Materials Eng.* **80** (1974) 48 op cit. in [46].

*Received 25 January 2002
and accepted 12 August 2003*